Journal of Engineering and Technology for Industrial Applications

ITEGAM-JETIA

Manaus, v.11 n.55, p. 222-229. September/October, 2025.
DOI: https://doi.org/10.5935/jetia. v.11 n.55.2666

ISSN ONLINE: 2447-0228

RESEARCH ARTICLE OPEN ACCESS

A DEEP LEARNING MODEL TO CLASSIFY FOREST FIRES BURNED AREAS USING SENTINEL-2 DATA IN ALGERIA.

OUAHAB Abdelwhab[1]

[1]Department of Mathematics and Computer Sciences, University of Ahmed Draia, Adrar, Algeria.

[1]https://orcid.org/0000-0003-0648-2947

Email: ouahab.abdelwhab@univ-adrar.edu.dz

ARTICLE INFO

Article History
Received: September 4, 2025
Revised: September 30, 2025
Accepted: October 6, 2025
Published: October 31, 2025

Keywords:
Deep learnig,
CNN,
Algeria,
Burned,
Forest fires.

ABSTRACT

Transfer learning involves using pre-trained CNN models, originally trained on large datasets like ImageNet, and fine-tuning them for specific tasks with smaller datasets. In this research, six pre-trained CNN models—VGG16, VGG19, DenseNet121, InceptionResNetV2, MobileNet, and MobileNetV2—were evaluated on a dataset comprising 30 plant species. The goal is to determine which transfer learning model performs best for plant species recognition. The forest fires in Algeria had a great impact on the public, economic, and environmental levels. Estimating the burned areas caused by this fire is essential. In this study, we suggest a new methodology based on deep learning using sentinel-2 images to classify the burned area that occurred in Algeria in 2022. This methodology uses a convolution neural network (CNN) to learn and classify the Sentinel-2 images into burned and unburned areas. The inputs of the proposed model are generated by calculating some spectral indices used in detecting the burned area. We measure the performance of the proposed model using accuracy, rappel, precision, and f1-score. The proposed method gives an accuracy of 0.97. We show that the proposed method has a high performance in detecting and classifying the burnt area.

I. INTRODUCTION

Fire is one of the most important factors that lead to damage to the environment and climate change. Every year, many forests are exposed to fires in different countries of the world [1]. This damage affects the physical and chemical properties of the soil, biodiversity, soil fertility, air purity, and other environmental impacts [2]. It is difficult to assess those affected by fires and to identify precisely burned areas due to the large temporal and spatial variability and uncertainty of fire occurrence [3]. Currently, remote sensing techniques are widely used to monitor changes on the Earth's surface and assess the impact of these changes on the environment by providing rapid information to determine fire-damaged areas in an accurate and appropriate way [4], [5]. These techniques have a lot of benefits compared to traditional techniques, including a large coverage and multiple temporal and spatial scales [2]. This is due to its ability to produce reliable and fast results, as well as its capacity to rapidly identify burnt areas for post-fire rehabilitation activities [6]. It is difficult to accurately determine the extent of fire damage and the severity of the burn by using ground measurements only due to the high variability and uncertainty of forest fires spatially and temporally [7].

Satellite sensors that are multispectral, such as Sentinel-2 satellite and Landsat series utilize medium-to-high spatial resolution to offer dependable data with a high temporal resolution [8], [9]. Several recent studies have shown that various spectral bands are sensitive to significant changes in spectral radiance in response to burning. These spectral bands can detect burnt areas, burn severity, and vegetation changes with reliability. For instance, thermal bands, mid-infrared and near-infrared are sensitive to burn magnitude changes and are commonly used for fire effects studies in vegetated areas [7]. In this sense, spectral indexes have been used for detecting burnt areas such as the Normalized Burned Raio (NBR) index [10], the Normalized Difference Vegetation Index (NDVI) [11], and the Soil-adjusted vegetation index [12]. The issue with these methods is that they may not perform effectively under varying weather conditions. Furthermore, the utilization of indices to identify fire damage typically necessitates manual or semi-manual techniques, which involve setting thresholds that are dependent on the soil type and cannot be easily established [13]. In recent times, deep learning methods have

been utilized in various applications with significant achievements, and their popularity is increasing in diverse fields. The generality of deep learning architectures allows them to be used for a broad range of classification tasks. As a result, similar architectures are being increasingly utilized for multi-label classification [14], among of them estimation, classification, and detection of burnt area. One of the major challenges in developing a deep learning model for burned areas is the limited access to training data [13]. The availability of free data from the Sentinel-2 satellite had a great role in monitoring the Earth and fires [4]. In recent years, Algeria has witnessed a terrible increase in the number of forest fires. This rise can be related to the effects of global warming and change in weather patterns [8]. It could also be due to criminal acts. These fires caused the loss of property and lives. Therefore, it has become necessary to predict these fires, know their causes, and estimate the extent of the damage they have caused. In this study, we suggest a new technique based on deep learning to classify and estimate the burned area using Sentinel-2 images. This approach has a high capacity for estimating the burned area. The used images are provided before and after the fire. We will exploit the various data generated by the various indices for the detection of burned areas to feed the deep learning model.

II. MATERIALS AND METHODS

The Sentinel-2A and Sentinel-2B satellites were respectively launched and put into orbit, in 2015 and 2017. The Sentinel-2 images consist of 13 spectral bands that cover the Visible, Near-Infrared (NIR), and Short-Wave Infrared (SWIR) ranges, with spatial resolutions of 10, 20, and 60 meters [8]. Sentinel-2 is frequently updated with a temporal frequency of 5 days. Table 1 displays the spatial and spectral characteristics of the satellite images obtained by Sentinel-2.

Table 1: Sentinel-2 bands with their spatial and spectral characteristics.

Band number	Wavelength	Spectral name	Spatial Resolution
B1	443	Coastal Aerosol	60
B2	490	Blue	10
B3	560	Green	10
B4	665	Red	10
B5	705	Red EDG-1	20
B6	740	Red EDG-2	20
B7	783	Red EDG-3	20
B8	842	NIR	10
B8a	865	Narrow NIR	20
B9	945	Water Vapor	60
B10	1375	Cirrus	60
B11	1610	SWIR-1	20
B12	2190	SWIR-2	20
TCI	RGB	RGB	10

Source: Authors, (2025).

All data used in the study are provided by the Sentinel-2B satellite. We used two types of data from the same area: data before the fire and data after the fire. The research area is located in Northeastern of Algeria which had a fire in August 2022. This area is illustrated in Fig. 1. The post-fire and pre-fire were chosen close to each other in order to reduce the spectral variance as a result of climate change. The pre-fire image was provided on the 12th of August 2022, and the post-fire image was provided on the 21st of August 2022. Both of the two selected images are free of clouds and fog [14].

Figure 1: Location of the study area (Algeria).
Source: Authors, (2025).

II.1 THE PROPOSED METHOD

The proposed method uses Sentinel-2B images, before and after the fire, to classify their pixels into burned and unburned pixels. All bands are resampled to 20 m in order to make them the same size. In our tasks, Convolution Neural Network (CNN) is used to classify the whole image. We generate a vector of nine values V from each pixel. This vector is considered as input for CNN. The nine values are calculated using some of the most well-known indices that are sensitive to burning.
There are no single spectral indices that can be universally effective in all environments. The used indices are:

II.1.1 NBR (Normalized Burn Ratio)

The NBR [6] is an index that detects burnt areas by analyzing the variations in the way burnt green vegetation and unburned green vegetation absorb and reflect light. It is computed using two specific Sentinel-2 bands which are Band 8 and Band 12. The equation of NBR is computed as follows [15]:

$$\mathrm{NBR} = \frac{B_8 - B_{12}}{B_8 + B_{12}} \tag{1}$$

The NBR takes values between -1 and 1. If the value of this indices is close to one, this means that the vegetation is not burnt and is in good health, while if the indices is close to -1, this means that the vegetation may be burnt or its health is not good.

II.1.2 dNBR (differenced Normalized Burn Ratio)

The dNBR indices is an effective tool for identifying the extent of burned areas and the severity of the burns. It takes positive values for burned areas and negative values for unburned areas [6].

$$\mathrm{NBR} = \frac{B_8 - B_{12}}{B_8 + B_{12}} \tag{2}$$

II.1.3 NDVI (Normalized Difference Vegetation Index)

The NDVI is the most important indices. It is used to extract vegetation areas [16]. It can be calculated using the bands 4 and 8 as follows:

$$\mathrm{NDVI} = \frac{B_8 - B_4}{B_8 + B_4} \tag{3}$$

NDVI takes values from -1 to 1, positive values corresponding to vegetation areas.

II.1.4 GNDVI (Green Normalized Difference Vegetation

This is indices is used to determine stressed vegetation. It is very sensitive to chlorophyll variation. It is calculated using the green band (B_3) and the near infrared (B_8) as follows [17] :

$$\mathrm{GNDVI} = \frac{B_8 - B_3}{B_8 + B_3} \tag{4}$$

The proposed model contains 3 CNNs. The first CNN is used to feed vectors generated from pre-fire image. The second CNN is used to feed data from post-fire image. The last CNN is used to combine the last result of the convolution layers of CNN-1 and CNN-2. CNN-1 and CNN-2 are used to extract the features from images before and after the fire. CNN-1 and CNN-2 have similar layers. The structure of CNN-1, CNN-2 and CNN-3 is shown in Table 2. The flowchart of the proposed model is shown in Fig.2.

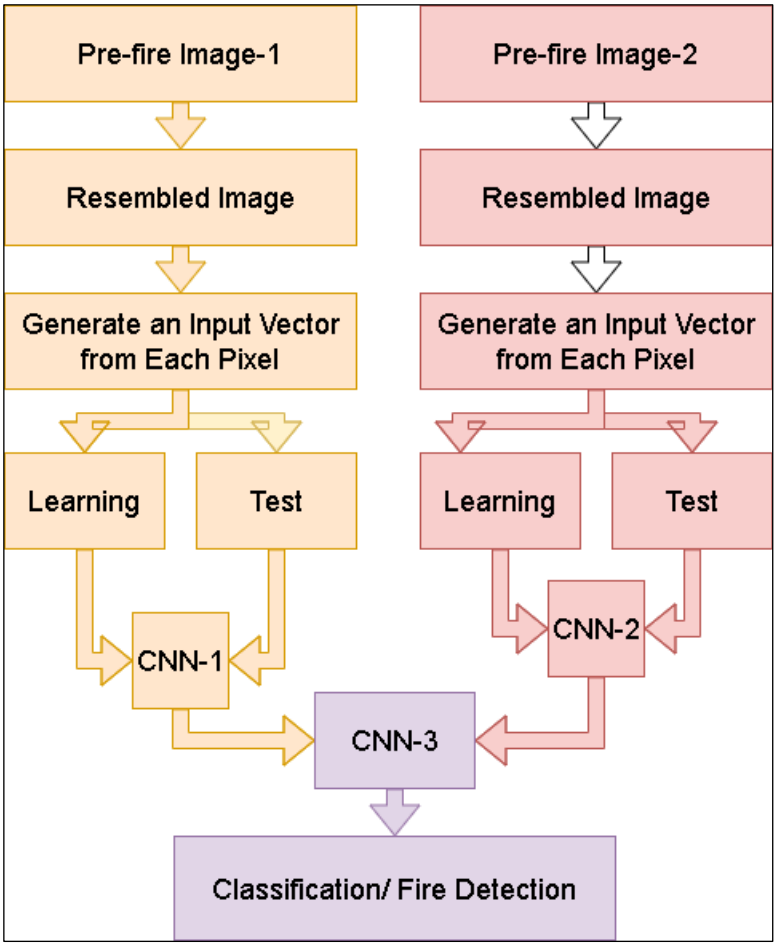

Figure 2: Flowchart of the proposed modal.
Source: Authors, (2025).

In order to perform the deep learning process, we select some pixels from the burned and unburned areas of the image under study. By using images before and after the fire, it is possible to discover in an automatic way the difference between the characteristics in the burned and unburned areas. After that, we calculate the various indices of fire detection corresponding to each pixel to form a vector of nine values that are used to feed the proposed model.

Table 2: The architecture of CNN-1, CNN-2 and CNN-3.

CNN-1 and CNN-2			
	Layer	**Kernel size**	**activation**
input	3*3*3		
Conv2D	16	3x3	relu
Conv2D	16	3x3	relu
MaxPooling2D		2x2	
Dropout(0.2)			
Conv2D	32	3x3	relu
Conv2D	32	3x3	relu
MaxPooling2D		2x2	
Dropout(0.2)			
Conv2D	64	3x3	relu
Conv2D	64	3x3	relu
MaxPooling2D		2x2	
Dropout(0.2)			
Flatten()			
CNN-3			
	Layer	Kernel size	activation
input	[FC1 FC2]		
Dense	64		relu
Dropout(0.2)			

Source: Authors, (2025).

The aim of using several indices instead of using one is to benefit from the characteristics of each index in detecting fire. We have determined the form of the input vector experimentally after a lot of tests and combinations. The structure of this vector is shown in Table 3.

Table 3: The structure of input vector.

NBR	NDVI	GNDVI	dNBR	NBR	NDVI	GNDVI	dNBR	dNBR

Source: Authors, (2025).

III. EXPERIMENT AND RESULTS

The experiment was carried out using TensorFlow and the Python 3.7 platforms. In our experiment, we selected 44418 pixels from the burned area and 44418 pixels from the unburned area. These pixels are used to train the proposed model. 66018 pixels are used to test the model. Half of them were taken from the burnt areas and the other half were taken from the unburned areas. Due to the lack of reference data in order to evaluate the validity of the proposed CNN model, a set of metrics are computed, which are the accuracy, precision, recall, F1-score, and loss function.

$$\text{Accurancy (A)} = \frac{\text{TP} + \text{TN}}{\text{TP} + \text{TN} + \text{FP} + \text{FN}} \tag{5}$$

$$\text{Precision (P)} = \frac{\text{TP}}{\text{TP} + \text{FP}} \tag{6}$$

$$\text{Recall (R)} = \frac{\text{TP}}{\text{TP} + \text{FN}} \tag{7}$$

$$\text{F1} - \text{Score (F1)} = 2 \times \frac{\text{P} \times \text{R}}{\text{P} + \text{R}} \tag{8}$$

TP : The number pixels of burned area classified as burned pixels, FP : The number pixels of burned area classified as unburned pixels. TN: The number pixels of unburned area classified as unburned pixels. FN : The number pixels of unburned area classified as burned pixels. The classified image is shown in figure 3.

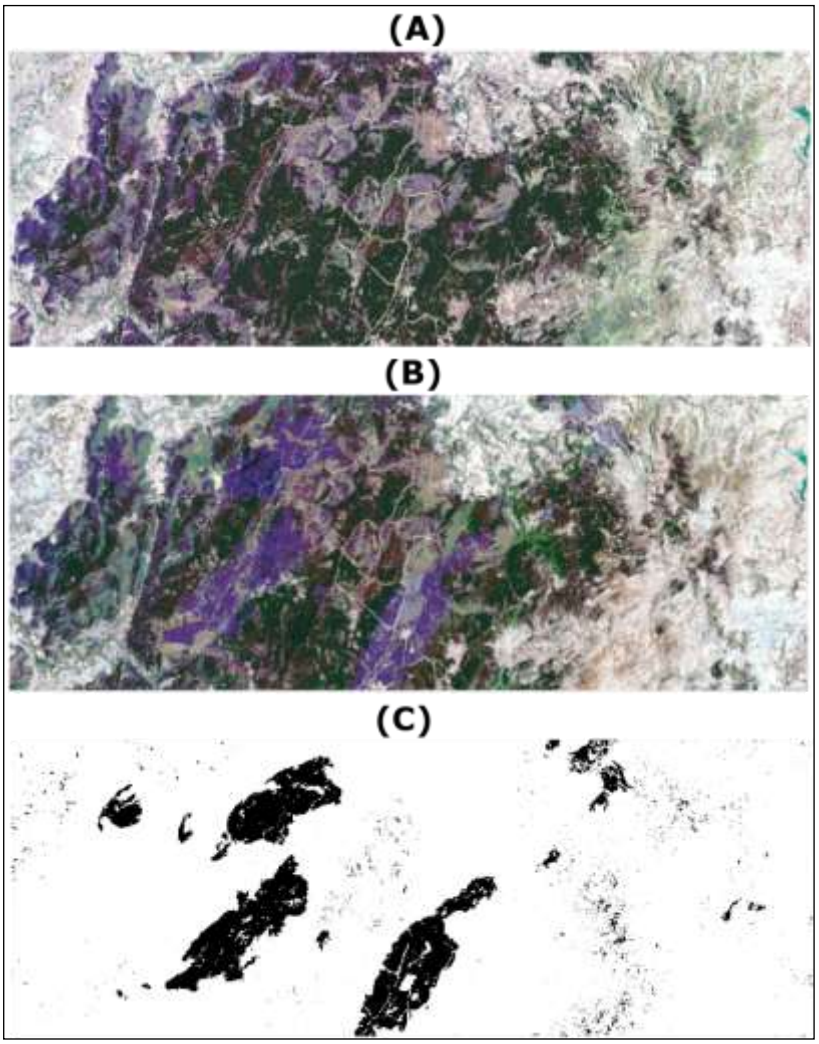

Figure 3: The sentinel-2 images of study area and its classification a) Image before the fire. b) Image after the fire c) the classified image using the proposed model.
Source: Authors, (2025).

Figure 4 and Figure 5 show the accuracy and loss functions for the proposed model that runs 100 iterations. It can be seen that the loss function decreases gradually and the accuracy function decreases gradually as the number of iterations increases. The accuracy values stabilize at 0.993. This indicates that the proposed model has a good performance.

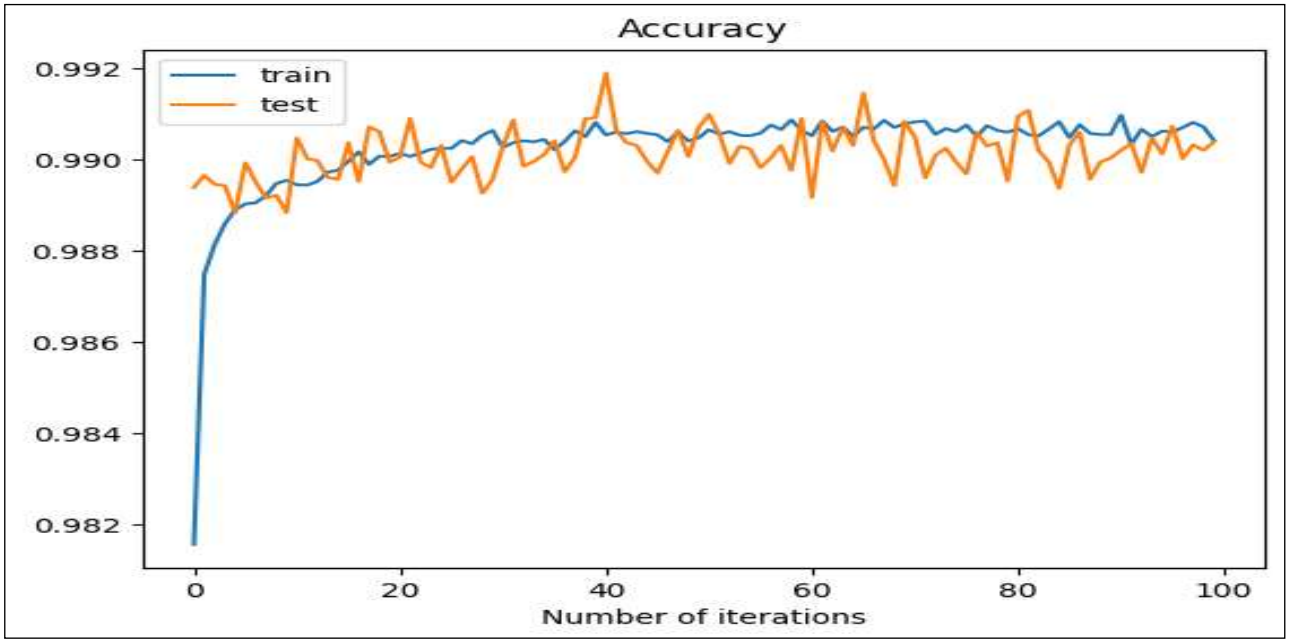

Figure 4: The accuracy functions of test and training abtained by the proposed model.
Source: Authors, (2025).

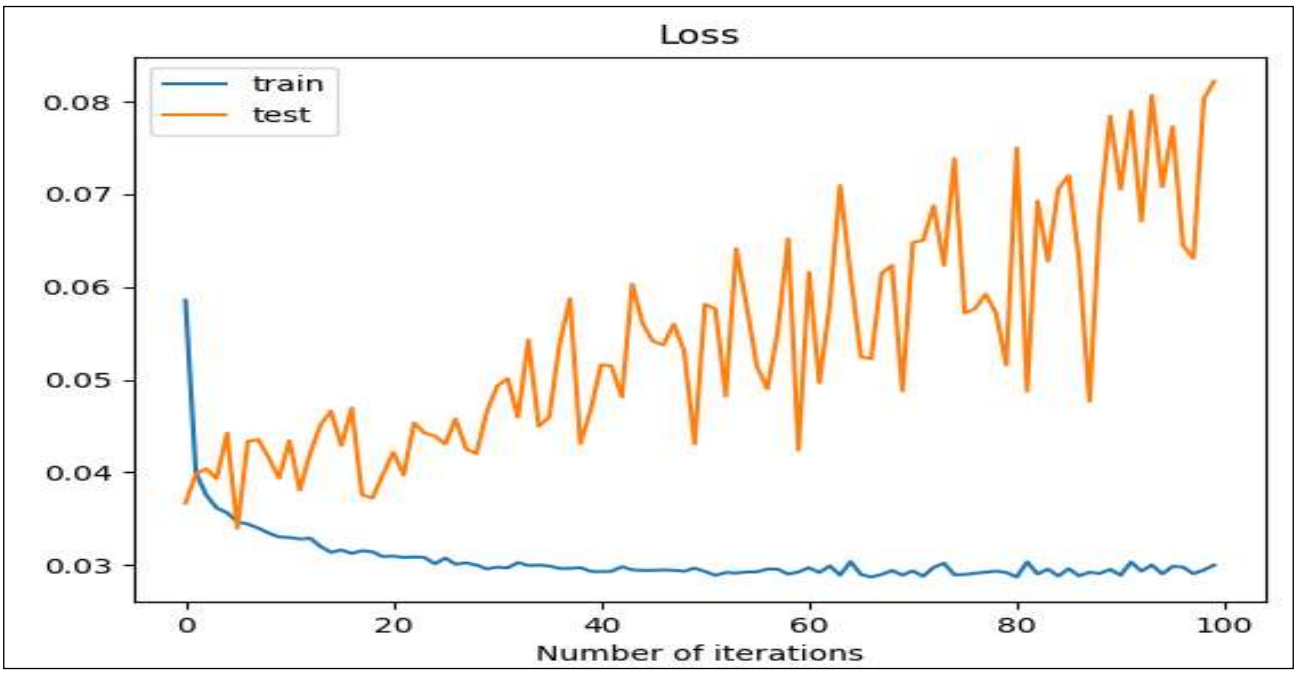

Figure 5: The loss functions of test and training abtained by the proposed model.
Source: Authors, (2025).

From Table 4, it can be seen that the precision is 0. 976. This can explain by the capacity of the proposed model to classify burned areas correctly. The value of accuracy is 0.98. This can be explained by the capacity of the proposed model to classify burned and unburned areas.

Table 4: Evaluation metrics.

Precision	Accuracy	Recall	F1-Score
0.976	0.98	0.97	0.97

Source: Authors, (2025).

Table 5 shows the confusion matrix obtained. In this matrix, the diagonal shows the number of pixels that are correctly classified. The others show the number of pixels that are incorrectly classified. It is noted that 96.7 % of burned pixels are correctly classified. The proposed model gives an error of 3.3% in estimating the burned areas.

Table 5: The confusion matrix.

Desired class % / Found class %	Burned pixels	Unburned pixel
Burned pixels	31919 (96.7%)	1090 (3.3%)
Unburned pixels	226 (0.69%)	32783 (99.31%)

Source: Authors, (2025).

IV. CONCLUSIONS

In the present work, we proposed a new methodology to classify the burned area using sentinel-2 images. The study area depends on the fire that happened in October 2022 in Algeria. We used a CNN with two inputs in order to enter inputs generated from images before and after the fire. The inputs are generated from the used data by computing some spectral indices, which are NDI, NBR, dNBR, and GNDVI. The performance of the proposed model is computed using accuracy, rappel, precision, and f1-score. The proposed method gives an accuracy of 0.97. This indicates that the proposed method has a high performance in classifying the burnt area.

V. AUTHOR'S CONTRIBUTION

Conceptualization: OUAHAB Abdelwhab.
Methodology: OUAHAB Abdelwhab.
Investigation: OUAHAB Abdelwhab.
Discussion of results: OUAHAB Abdelwhab.
Writing – Original Draft: OUAHAB Abdelwhab.
Writing – Review and Editing: OUAHAB Abdelwhab.
Resources: OUAHAB Abdelwhab.
Supervision: OUAHAB Abdelwhab..
Approval of the final text: OUAHAB Abdelwhab.

VI. REFERENCES

[1] T. Seyd, H. Mahdi, and C. Jocelyn, "Burnt-Net: Wildfire burned area mapping with single post-fire Sentinel-2 data and deep learning morphological neural network," Remote Sens., vol. 140, pp. 1–10, 2022.

[2] H. Luo and J. Wu An, "Assessment of the suitability of Sentinel-2 data for identifying burn severity in areas of low vegetation," J. Indian Soc. Remote Sens., 2022. [Online]. Available: https://doi.org/10.1007/s12524-022-01518-7

[3] X. Chen, J. E. Vogelmann, M. Rollins, D. Ohlen, C. H. Key, L. Yang, C. Huang, and H. Shi, "Detecting post-fire burn severity and vegetation recovery using multitemporal remote sensing spectral indices and field-collected composite burn index data in a ponderosa pine forest," Int. J. Remote Sens., vol. 32, no. 23, pp. 7905–7927, 2011.

[4] P. Zhang, X. Hu, and Y. Ban, "Wildfire-S1S2-Canada: A large-scale Sentinel-1/2 wildfire burned area mapping dataset based on the 2017–2019 wildfires in Canada," in Proc. IGARSS 2022 - IEEE Int. Geosci. Remote Sens. Symp., pp. 7954–7957, Jul. 2022, doi: 10.1109/IGARSS46834.2022.9884275.

[5] F. Filipponi, "Exploitation of Sentinel-2 time series to map burned areas at the national level: A case study on the 2017 Italy wildfires," Remote Sens., vol. 11, no. 6, pp. 622, Mar. 2019.

[6] R. Lorens, J. A. Sobrino, C. Fernández, J. Fernández-Alonso, and J. A. Vega, "A methodology to estimate forest fires burned areas and burn severity degrees using Sentinel-2 data: Application to the October 2017 fires in the Iberian Peninsula," Int. J. Appl. Earth Obs. Geoinf., vol. 95, pp. 102243, Jan. 2021.

[7] H. Farhadi, M. Mokhtarzade, and H. Ebadi, "Rapid and automatic burned area detection using Sentinel-2 time-series images in Google Earth Engine cloud platform: A case study over the Andika and Behbahan regions, Iran," Environ. Monit. Assess., vol. 194, pp. 369, Jun. 2022.

[8] M. Zanetti, "A high resolution burned area detector for Sentinel-2 and Landsat-8," in Proc. 10th Int. Workshop Analysis of Multitemporal Remote Sensing Images (MultiTemp), Shanghai, China, pp. 1–4, Jul. 2019, doi: 10.1109/Multi-Temp.2019.8866958.

[9] W. Chen, K. Moriya, T. Sakai, L. Koyama, and C. X. Cao, "Mapping a burned forest area from Landsat TM data by multiple methods," Geo. Hazards Risk, vol. 7, no. 1, pp. 384–402, Mar. 2014.

[10] A. R. Huete, H. Q. Liu, K. Batchily, and W. Leeuwen, "A comparison of vegetation indices global set of TM images for EOS-MODIS," Remote Sens. Environ., vol. 59, pp. 440–451, 1997.

[11] A. M. Al-Dabbagh and M. Ilyas, "Uni-temporal Sentinel-2 imagery for wildfire detection using deep learning semantic segmentation models," Geo. Nat. Hazards Risk, vol. 14, no. 1, pp. 1–15, 2023.

[12] O. Abdelwhab, "Multimodal convolutional neural networks for detection of COVID-19 using chest X-ray and CT images," Opt. Mem. Neural Netw., vol. 30, pp. 276–283, Jul. 2021.

[13] R. Zennir and B. Khallef, "Forest fire area detection using Sentinel-2 data: Case of the Beni Salah national forest Algeria," J. For. Sci., vol. 69, no. 1, pp. 1–10, 2023.

[14] K. Choudhary, W. Shi, and M. S. Boori, "Agriculture phenology monitoring using NDVI time series based on remote sensing satellites: A case study of Guangdong, China," Opt. Mem. Neural Netw., vol. 28, pp. 204–214, Mar. 2019.

[15] G. Navarro, I. Caballero, G. Silva, P. Parra, A. Vázquez, and R. Caldeira, “Evaluation of forest fire on Madeira Island using Sentinel-2A MSI imagery,” Int. J. Appl. Earth Obs. Geoinf., vol. 58, pp. 97–106, Feb. 2017.

[16] A. Craig, P. George, and F. Konstantinos, “Determining the use of Sentinel-2A MSI for wildfire burning and severity detection,” Int. J. Remote Sens., vol. 40, no. 3, pp. 905–930, Feb. 2018.

[17] M. Rahman, L. Di, E. Yu, L. Lin, C. Zhang, and J. Tang, “Rapid flood progress monitoring in cropland with NASA SMAP,” Remote Sens., vol. 11, no. 2, pp. 1–15, Jan. 2019.